JOURNAL OF Materials Feature Article CHEMISTRY

LCD components obtained by patterning of chiral nematic polymer layers

Peter van de Witte,* Martin Brehmer† and Johan Lub

Philips Research Laboratories, Prof. Holstlaan 4, 5656 AA Eindhoven, The Netherlands. E-mail: witte@natlab.research.philips.com

Received 31st March 1999, Accepted 7th May 1999

An overview is given of the methods for preparation of birefringent films with patterned optical properties and their applications in liquid crystal displays. A versatile method of obtaining patterned films is based on manipulation of the helical twisting power of chiral dopants by photoisomerization reactions. Because of their transparency to visible light, high helical twisting power and large changes of the helical twisting power during UV irradiation, menthone derivatives are very suitable dopants for this process. A number of potential applications of the principles are discussed. Patterning of chiral nematic films with regions with different twisting angles is a suitable method for the preparation of patterned polarization rotators. Patterning of chiral nematic liquid crystal layers can also be used to control the reflection color and state of polarization of the reflected light. Such layers are useful for the preparation of reflective color filter arrays and broad band reflective polarizers.

1. Introduction

1.1. Optical films in LCDs

Many polymer based optical films are currently used in both active matrix and passive matrix twisted nematic liquid crystal displays (LCDs).[1] For a long time the classical absorption based polarizer and analyzer were the only optical films in a LCD. More recently other films with new functionalities have been introduced in LCDs (see Table 1). Brightness enhancement films and reflective polarizers are used to improve the light efficiency of LCDs. Compensation films and retarders are used to improve the angular and spectral dependence of the viewing angle properties. Front scattering films and holographic films are components that are attracting interest for application in reflective displays. A common feature of these films is that they have to perform complicated optical functions. A dedicated production technology is usually required to obtain films with the desired properties.

At this moment, all of these optical films have uniform optical properties across the surface area. For some applications, however, it is useful to locally tailor the optical properties. Examples of such applications are patterned polarization rotators for stereoscopic displays, polarization sensitive gratings, reflective color filters and patterned polarizers. Recently, a number of new technologies based on the manipulation of the organization of liquid crystals have become available that allow the preparation of such structured films. Some of the most promising technologies are based on manipulation of the orientation of liquid crystals by light.

†*Present address*: University of Wuppertal, Dept. of Chemistry and Institute of Materials Science, BUGH Wuppertal, Gauss Str. 20, D42097, Germany.

1.2. Methods of obtaining structured birefringent films

A first method that can be used is based on controlling the alignment of liquid crystals. To obtain a long-range orientation of liquid crystals alignment layers are required. In the production process of LCDs this alignment is achieved by rubbing thin layers (50–100 nm) of polyimides with a velvet cloth.[20] This rubbing process is known to generate dust and static electricity. Therefore, much effort is being dedicated to developing an alternative process.

Photoalignment is a promising alternative process to rubbing. During the photoalignment process a polymer alignment layer is irradiated with polarized light. For certain materials this polarized light can give rise to rupture or combination of bonds in a specific direction. On the treated alignment layer the liquid crystals can orient either parallel or perpendicular to the plane of polarization of light used for the exposure. Examples are the UV light induced cycloaddition of cinnamate and coumarin derivatives and the photodegradation of polyimides.[21–23] A second possibility is to use dye-doped orientation layers. Especially dyes capable of *cis–trans* isomerization show a fast reorientation perpendicular to the plane of polarization of incident light.[24–27] Photoisomerizable liquid crystalline surfactants can be used to achieve similar effects ('command surfaces').[28] Apart from offering an alternative to the rubbing process, these processes also open new possibilities of making structured birefringent layers. By locally controlling the polarization direction of the light used for structuring, the alignment direction can be adjusted. When a liquid crystal or a liquid crystalline polymer is deposited on top of the structured alignment layer, a birefringent layer with a locally varying optical axis can be obtained.[29,30]

For some applications it is advantageous to control the twist angle of liquid crystals rather than the optical axis of non-twisted liquid crystals. For example, this would make structuring of the properties of cholesteric liquid crystals possible. None of the above mentioned methods offers that possibility. Recently, a new method for locally varying the properties of liquid crystalline layers was demonstrated.[31–33] This method is based on photo-induced manipulation of the helical twisting power of chiral dopants and will be the main topic of this contribution.

1.3. Photo-induced modification of the helical twisting power of chiral dopants

Chiral molecules are added to liquid crystals to control the twisting sense and the rotation angle of the layer.[20] The distance over which the molecules rotate 360° is called the pitch (P). The effectiveness of chiral molecules in rotating the liquid crystals is given by the helical twisting power (HTP) [eqn. (1)],

$$HTP = \frac{1}{P \times c} \quad (1)$$

Table 1 Examples of optical films used in liquid crystal displays

Name	Function	Structure	Process	Refs.
Brightness enhancement films	Improve light efficiency (collimation of light)	Surface profile	Embossing Replication	2
Reflective polarizers	Improve light efficiency (light recycling)	Pitch gradient cholesteric layer Special polymer blends	Photopolymerization of liquid crystals Extrusion/stretching	3,4,5,6
Light control films, holographic films	Control specular reflection	Inclined gratings Scattering layers	Photopolymerization Embossing	7,8,9
Retarders	Minimize wavelength dependence STN	Birefringent films	Stretching Spincoating Photopolymerization of liquid crystals	10,11, 12,13, 14,15
Compensation films	Minimize viewing angle dependence	Birefringent films with inclined optical axis	Photopolymerization of liquid crystals	16,17, 18,19

in which *c* represents the concentration of the chiral molecule. The *HTP* is known to be strongly dependent on the conformation and chemical structure of the chiral liquid crystal. When the conformation or the chemical structure of the molecules is changed by light, the *HTP* of the molecules will also be influenced. For instance, photodegradation of chiral groups can be used to manipulate the *HTP* of chiral compounds. Recently, the photoracemization of binaphthyl derivatives was demonstrated by Chien and coworkers.[34] In this process optically active molecules are converted by intense UV irradiation to racemic mixtures of the isomers with no net *HTP*. Similar effects using photoinduced ring closure reactions and racemization reactions were reported by Yokoyama *et al.*[35] A particularly efficient method is to make use of photoisomerization reactions. For most photoisomerizable chiral compounds the *E*- and the *Z*-isomers will have different helical twisting powers. Feringa *et al.* and Schuster *et al.* developed special photochemical isomerization reactions to influence the helical twisting power of chiral compounds.[36–38] We recently demonstrated that the isomers of chiral stilbenes also have a different *HTP*.[31]

For application of photoisomerizable materials in optical components several additional material properties are desired: (1) the materials should be transparent to visible light, (2) large changes in helical twisting power during irradiation should be possible, (3) the mixture obtained after irradiation should be stable in time, (4) the materials should have a broad temperature range for the chiral mesophase, (5) a large pitch range should be accessible.

Recently, it was reported that menthone derivatives give a large shift of the *HTP* upon *E–Z* isomerization.[33,39–41] Their *HTP* is attractive, because reflection of visible light can be achieved with low concentrations of chiral material. Furthermore the compounds are transparent and non-reisomerizable at room temperature. Here we will investigate the details of the photoisomerization of menthone derivatives and the application of these compounds in optical films and components for LCDs.

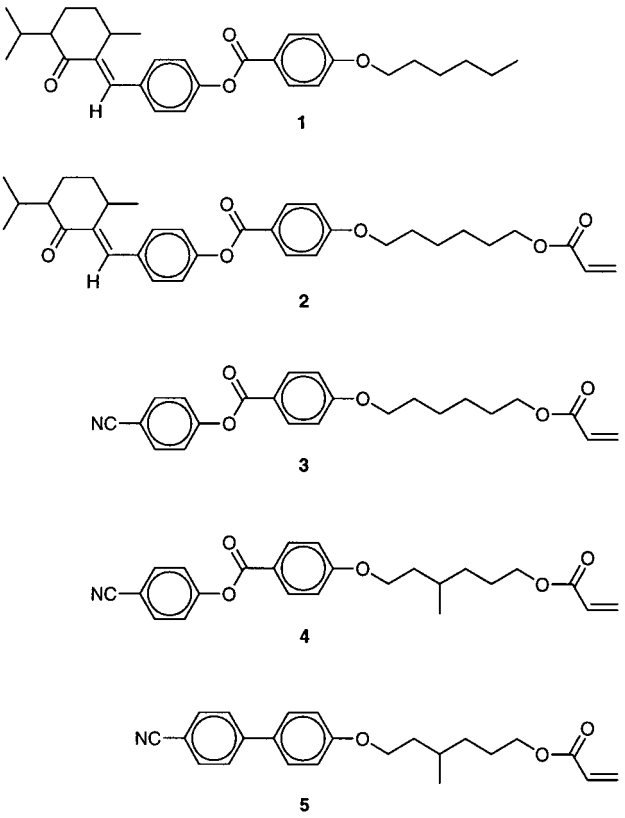

Fig. 1 Chemical structures of the compounds.

2. Materials

2.1. Synthesis

The chemical structures of the compounds are shown in Fig. 1.

The photoactive dopants **1** and **2** are derived from menthone. In order to make a molecule which is compatible with liquid crystals, a semi mesogenic group containing two aromatic rings and a spacer group was connected to the menthone unit (monomer **1**).[31] Monomer **2** contains the photoisomerisable vinylic unit of which the synthesis is described in Scheme 1. The condensation between menthone and 4-hydroxybenzaldehyde was performed with a protected form of the aldehyde. Without protection the condensation was not possible. The synthesis of co-monomer **3** has already been described in the

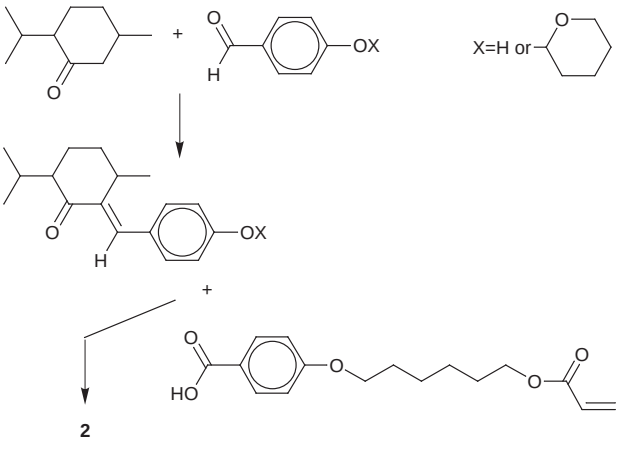

Scheme 1 Synthetic scheme for monomer **2**.

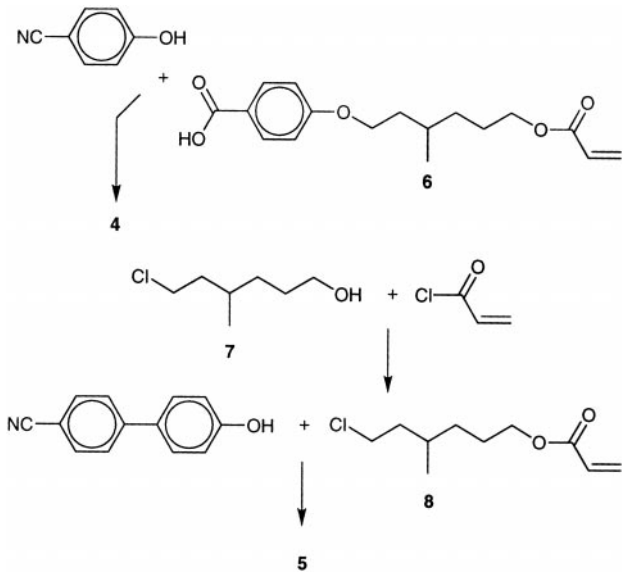

Scheme 2 Synthetic scheme for monomers **4** and **5**.

literature.[42] The co-monomers used for the synthesis of the polymers that increase their *HTP* with irradiation should contain a chiral monomer with opposite *HTP* compared to that of **2**. Monomers containing spacers derived from (*S*)-3-methyl-6-hydroxy-1-chlorohexane **7** show an *HTP* opposite to that of **2**.[43,44] For that reason, monomer **4** was designed and synthesised. Scheme 2 shows that it was made by esterification of 4-cyanophenol with the chiral acid **6**. The synthesis of **6** is described in a previous publication.[43] Another monomer derived from (*S*)-3-methyl-6-hydroxy-1-chlorohexane is **5**, a derivative of 4-hydroxy-4′-cyanobiphenyl (see Scheme 2). Both monomers form cholesteric polymers with more or less the same properties. Because of the ease of synthesis, monomer **5** was used for the synthesis of the copolymers instead of monomer **4**.

Polymers with different amounts of menthone derivative **2** were prepared by radical polymerisation (Table 2).[32] The molar mass was kept low by the addition of tetradecanethiol as a chain transfer reagent. In this way polymers with an M_n of 6000–7000 g mol^{-1} were obtained. Polymer **E** is the homopolymer of **2**. This polymer is not liquid crystalline (see Table 2). In order to make a chiral nematic polymer, a copolymer was synthesized using **2** and comonomer **3**. This last monomer is known to form a nematic side-chain polymer with a relatively broad nematic range.[45]

Table 2 Properties of the (co-)polymers

	x^a	Phase transitions[b]	β_p/μm^{-1} [c] (polymer chain)	β_m/μm^{-1} [c] (chiral unit)	β_i/μm^{-1} [c] (chiral unit irradiated[d])
		Copolymers of monomer **2** with monomer **3**			
A	0	g 23 N 113 I	—	—	—
B	0.15	g 18 N* 102 I	−2.5	−15.3	−2.9
C	0.33	g 18 N* 89 I	−6.6	−16.7	−2.8
D	0.50	g 35 I	−10.5	−18.1	−2.4
E	1	g 40 I	−14.9	−14.9	−1.4
		Copolymers of monomer **2** with monomer **5**			
F	0	g 12 N* 61 I	+4.8	—	—
G	0.07	g 20 N* 56 I	+3.0	—	+3.9
H	0.13	g 22 N* 67 I	+1.2	—	+2.8
I	0.22	g 24 N* 58 I	−1.7	—	+2.0

[a]Molar ratio of **2**. [b]Determined by DSC, g = glassy state, N = nematic, N* = cholesteric, I = isotropic. [c]Helical twisting power calculated from pitch measured in wedge cells (0.02–0.1 wt% polymer in E7, room temperature). [d]Irradiated at 365 nm (60 min, room temperature).

2.2. Thermal properties of the copolymers

As shown in Table 2, copolymers of menthone and up to 33% of **2** still resulted in polymers with chiral nematic phases. Higher fractions of **2** resulted in amorphous copolymers. The homopolymer of **5** exhibits a chiral nematic phase. In contrast, non-chiral analogues of **5** yield smectic polymers.[46] All synthesized copolymers of **2** and **5** also exhibited chiral nematic mesophases. The glass transitions of the polymers appear to increase somewhat with increasing menthone content.

2.3. *E–Z* isomerization

The menthone containing compounds can be isomerized from the *E*- to the *Z*-isomer during exposure to UV light. UV spectra of a solution of compound **1** in dichloromethane and in acetonitrile were recorded during irradiation.[31] The trends in the spectra were the same for both solvents. Fig. 2 shows only the results for dichloromethane.

The maximum of the absorption peak shifts to lower wavelengths. An isosbestic point was observed at 271.5 nm, indicating that also in this case side-reactions are limited. The results for **1** are in agreement with the results obtained by Yarmolenko *et al.* for a related compound.[39]

The *E–Z* isomerization was also monitored with the aid of proton NMR spectroscopy. The starting *E*-isomer exhibits the signal of the vinylic proton at 6.9 ppm (Fig. 3A). Upon irradiation this signal disappears and a new signal, typical of the vinylic proton of the *Z*-isomer, appears at 6.2 ppm (Fig. 3B). It shows a small amount of the starting *E*-isomer by the signals of the aromatic ring at 7.1 and 7.4 ppm. It can be concluded that a very clean isomerization is obtained.

Irradiated solutions of **1** in acetonitrile were analyzed using HPLC.[31] Fig. 4 clearly shows that the *E*-isomer rapidly converted to the *Z*-isomer. The conversion of **1** was essentially complete within 10 min.

The *HTP* (Table 2) of the polymers at room temperature is proportional to the amount of chiral monomer **2**. There appears to be no discernible effect of the composition of the polymer on the *HTP* of the chiral unit. Also the values for the low molecular weight compounds **1** and **2** are in the same range.[31] The polymers **A–E** show a large decrease of the absolute value of the *HTP* during photoirradiation indicating that the *HTP* of the *Z*-isomer is much lower than that of the *E*-isomer. When chiral comonomers are used with opposite

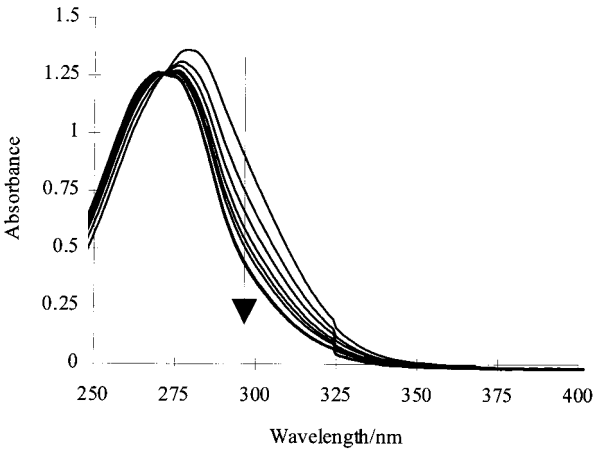

Fig. 2 UV spectra as a function of irradiation time for compound **1**. The lines represent (in the order indicated by the arrow): 0, 1, 2, 3, 4, 5, 10, 20, and 50 min of irradiation. Note that the lines for the longest irradiation time may overlap one another. Intensity UV light (365 nm): 8 mW cm^{-2}.

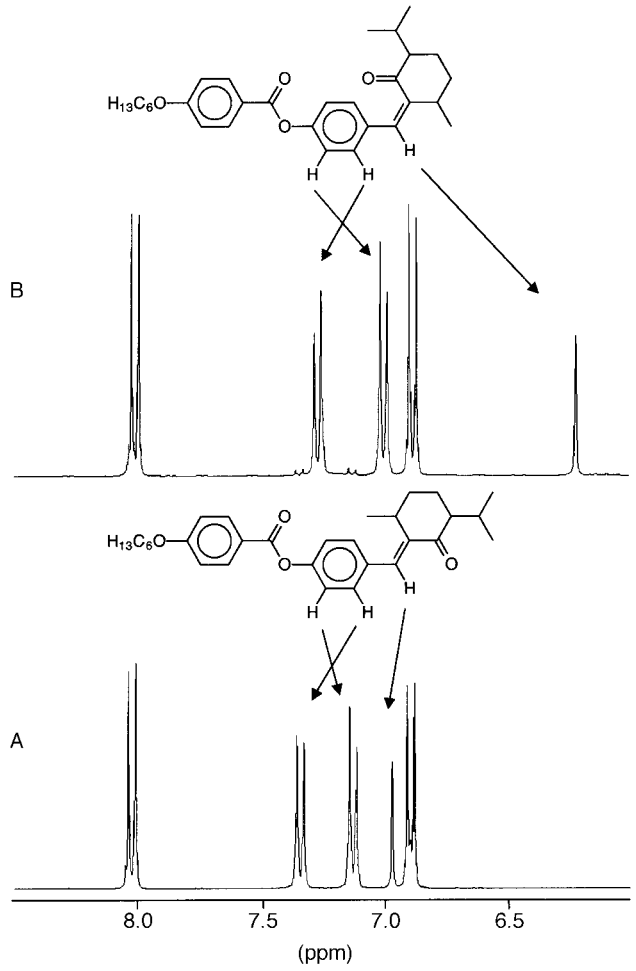

Fig. 3 NMR spectra of compound **1** (A) before and (B) after prolonged isomerization.

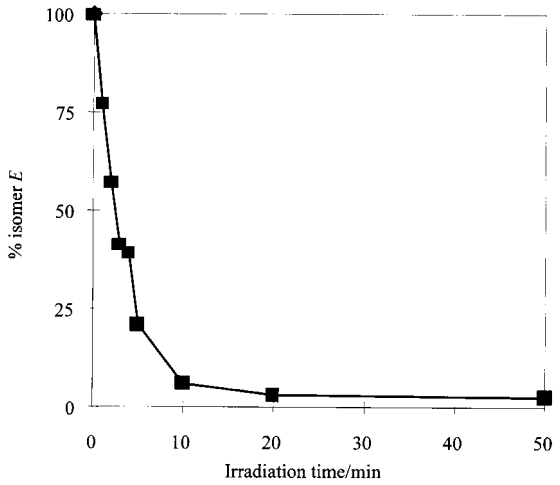

Fig. 4 Extent of isomerization as a function of UV exposure as measured by HPLC. Intensity UV light (365 nm): 8 mW cm^{-2}.

chirality (copolymers **F–I**) the dependence of the *HTP* during irradiation is more complex. This will be further discussed in section 4.3.

3. Application in twisted nematic layers[41]

Compound **1** was dissolved in small quantities in liquid crystalline polymer **A** (<3 wt%). After ageing below the clearing point well-oriented layers with a twisted nematic orientation could be obtained. Without UV exposure the *HTP* of the material dissolved in the polymer was measured to be $-27\ \mu m^{-1}$. As can be expected on the basis of the results described in the previous section, the *HTP* of **1** in the nematic polymer is dependent on the UV dose (Fig. 5).

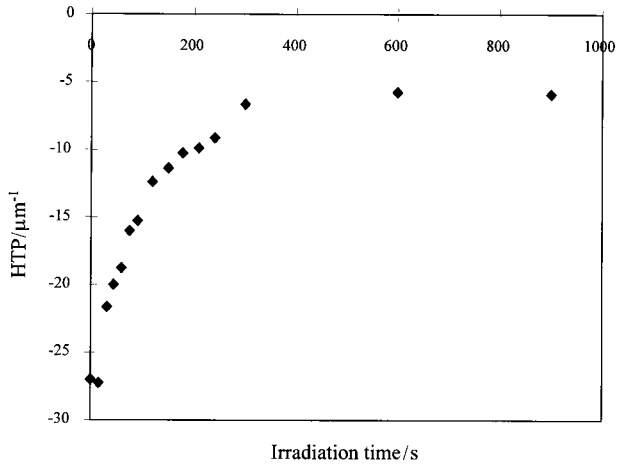

Fig. 5 Helical twisting power of **1** in **A** as a function of irradiation time. Concentration 1.3 wt% **1**. Intensity UV light (365 nm): 7 mW cm^{-2}.

The absolute value of the *HTP* of **I** decreases during UV exposure. Equilibrium is obtained after a UV dose of approximately 3 J cm^{-2} (400 s exposure). It is interesting to investigate the influence of these changes in *HTP* in chiral nematic layers with twist angles ranging between 0 and 90°. Between crossed polarizers such variations in twist angle will show up as large variations in light transmission. A 90° twist angle will lead to a high transmission of light. For minimum transmission a non-twisted retarder is required with its optic axis parallel or perpendicular to the polarizer axes.

From Fig. 5 it is clear that after irradiation the twisting power of the *Z*-isomer of the menthone derivative is not zero. Addition of a non-photosensitive chiral dopant with opposite twisting sense is required to compensate the residual twisting power. The commercially available R811 (Merck, Darmstadt, Germany) was used for this purpose. In Fig. 6 the measured twist angles in a 2.5 micron thick film obtained with a mixture of 0.3 wt% R811 and 0.5 wt% **1** in **A** are shown.

The twist angle before irradiation is close to the desired 90° while after 300 s of irradiation the twist angle is close to zero. Grey scale production is possible by using intermediate exposure times. A complex pattern containing grey scales was recorded in the polymer film using a UV illumination through a negative of a photograph. The results are shown in Fig. 7.

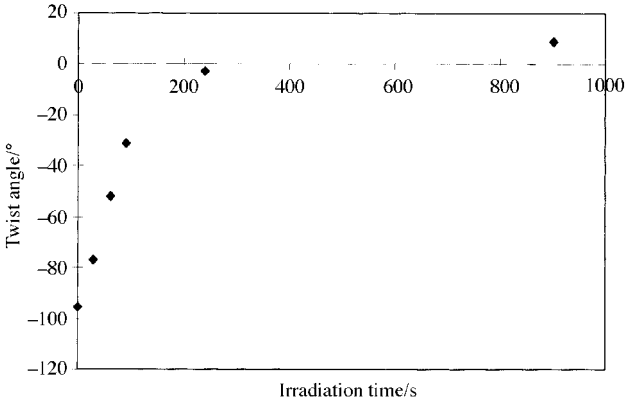

Fig. 6 Twist angle for a 2.5 micron thick film as a function of irradiation time. The composition is 0.3 wt% R811 and 0.5 wt% **1** in **A**. Intensity UV light (365 nm): 7 mW cm^{-2}.

Fig. 7 Reproduction of a negative of a photograph. Photograph of the sample between crossed polarizers.

It is clear that the reproduction of the figure in the layer is very good.

The black and white contrast is more than 20 and the transmission of the white state is more than 90% of the theoretical maximum.[41] The fact that the UV dose can be used to make grey scales is a major difference between this method and the earlier published method that is based on the reorientation of dyes in polarized light.[24] In the latter case the grey scales have to be produced by changing the polarization direction of the light.

One example of an application of these types of layers in liquid crystal displays is to use these structured layers for polarization encoded stereoscopic vision. It is well known that a 3D-impression from a display can be obtained when the left and right eye receive similar images that are slightly shifted in position with respect to each other. One of the methods of achieving this is to provide one of the images in one polarization state and the other image in the second polarization state. The information for both eyes is simultaneously present on the screen. The viewer needs glasses provided with two polarizers with orthogonal polarization directions to select the information for each of the eyes. The system is shown in Fig. 8.

The patterned chiral nematic layers can be used to display the information in the desired polarization. The display has to be provided with a polarizer to be able to generate polarized light. In case of an LCD this polarizer is always present. We have shown earlier that it is possible to pattern a chiral nematic film with areas that do not rotate the polarization of light and areas that rotate the polarization over 90°. When for example the odd data lines are provided with the parts of the retarder that rotate the polarization by 90°, and the even data lines are provided with the parts of the retarder that do not rotate the polarization of light, half of the display can be used to provide the information for one eye and the second half for the other eye. The here-described method is easier than the currently used systems based on photolithographic structuring of the polarizer.[47]

4. Modification of the periodicity of cholesteric liquid crystals[32]

Cholesteric liquid crystalline phases are well-known for their ability to reflect light.[48] The wavelength of maximum reflection (λ) and the width of the band depend on the pitch (P) of the

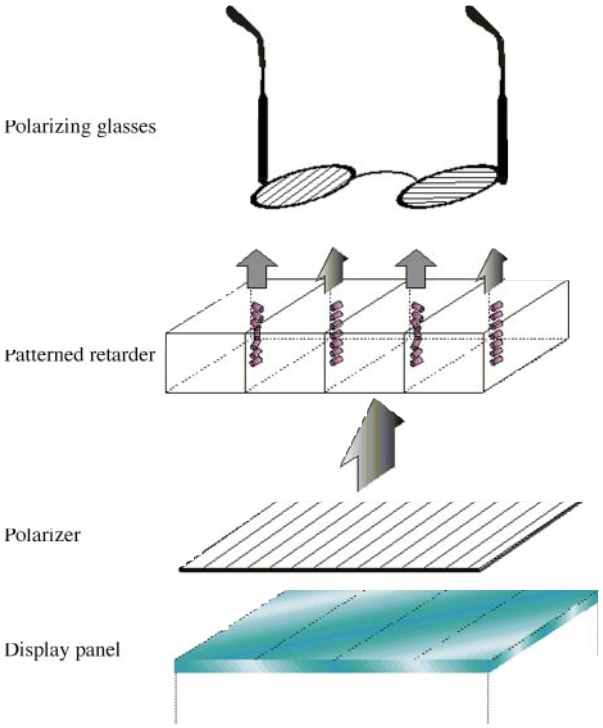

Fig. 8 Principles of polarization encoded stereoscopic vision.

cholesteric liquid crystal phase and the refractive indices (n_e and n_o) of the liquid crystals [eqn. (2) and (3)].

$$\lambda = P \times n \tag{2}$$

$$\Delta\lambda = P \times \Delta n \tag{3}$$

Here: n is the average refractive index of the film and Δn is the birefringence ($n_e - n_o$). When the reflection wavelength of a cholesteric liquid crystal is in the range of visible light, well-oriented layers of the cholesteric liquid crystals give rise to vivid iridescent colors. As can be expected for an interference effect, the color is angular dependent. For these reasons cholesteric liquid crystals are being studied for application as special pigments in paints.[49,50] The reflected light is circularly polarized. This means that these materials are also suitable for the preparation of polarization-sensitive optical components.[51]

Using photoisomerization of menthone derivatives it is possible to manipulate the periodicity of the helix. This technology would allow the preparation of cholesteric samples that reflect different colors in different areas. Three examples will be presented: (1) shifting of the position of the reflection band, (2) broadening of the reflection band and (3) changing the twisting sense.

4.1. Shifting of the position of the reflection band

Due to the large *HTP* of the menthone derivative **2**, copolymer **B,** containing only 15% of this derivative, still reflected UV light. The reflection color of the sample was dependent on the dose of UV light and could be changed from an ultraviolet to an infrared pitch. Due to the high viscosity the changes proceeded rather slowly: it took 15 min at 60 °C for the samples to change color. A gradual broadening of the reflection band with UV exposure could also be observed. Irradiated samples became more light scattering at prolonged exposure times. Both effects indicate a loss of orientation.

The solution of copolymer **C** in the low molar mass nematic liquid crystal host E7 (50% w/w) showed a similar behaviour upon irradiation (Fig. 9). The colors could be shifted over the whole visible spectrum. Due to the low viscosity of this mixture, the pitch changed instantaneously at room tempera-

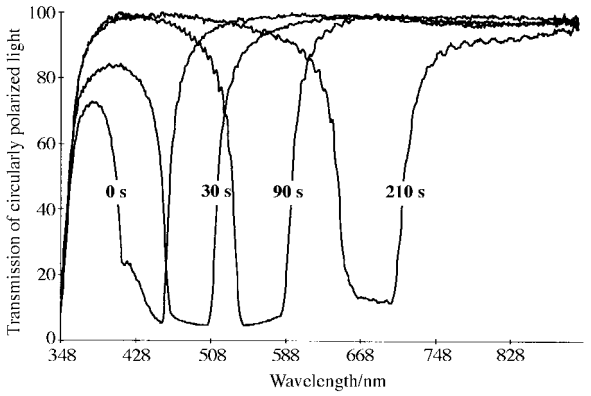

Fig. 9 Transmission spectra as a function of exposure time for samples prepared from a mixture of 50 wt% **C** and 50 wt% E7. Intensity UV light (365 nm): 5.6 mW cm^{-2}.

ture. There was no visible change of orientation. The reflected colors remained iridescent. The width of the absorption bands at half height is 60 nm and rises to 70 nm with increasing values for the pitch. The shape of the reflection band did not change. This indicates that the ordering of the liquid crystals remains good. In curve A of Fig. 12, the wavelengths of the boundaries of the reflection band are plotted against irradiation time. It shows a more or less linear increase in the reflection wavelength with irradiation time. From this figure the irradiation dose necessary for the different colors can be determined. In Fig. 10 a sample is presented that was obtained by local exposure of samples to various doses of UV light.

Color filters for reflective displays are a good application of this principle. Normally the red, green and blue color filters in LCDs are prepared *via* repeated lithographic procedures: which include for each color the sequence (1) coating, (2) partial exposure to UV light and (3) stripping. The positions of the color filters have to be carefully positioned with respect to each other. The technique described above allows an instant patterning of a cholesteric layer with the three desired colors. In addition, the cholesteric color filter integrates a reflection function, a polarizing function and a color function in one layer. For absorption based color filters three separate layers are required for these functions. The easiest way to obtain an array of cholesteric color filters is to expose a layer of cholesteric material *via* a patterned mask (Fig. 11).

After irradiation the part of the mask that is completely transmissive for UV light induced the red color in the film, the part of the mask that blocks UV light induced the blue color, and the part of the mask with intermediate transmission induced the green color.

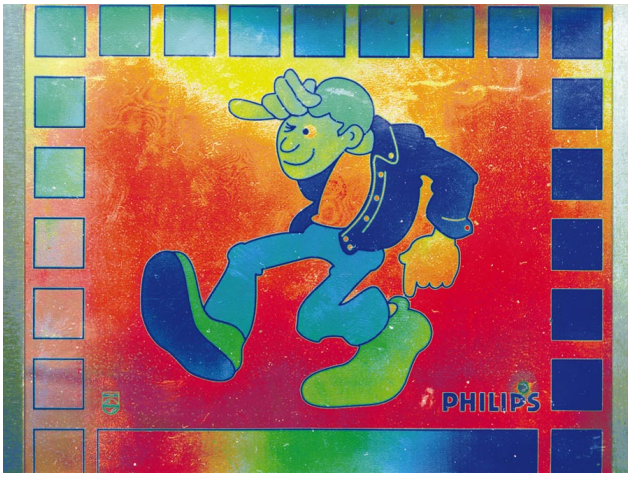

Fig. 10 Photograph of a sample patternwise exposed to UV light.

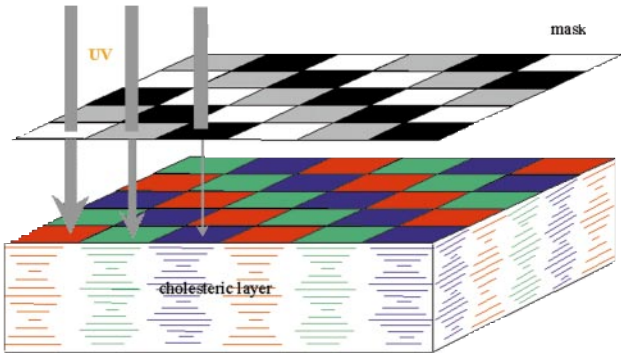

Fig. 11 Principles of one step manufacturing of reflective color filter arrays.

4.2. Broadening of the reflection band

Cholesteric layers will normally reflect only light with wavelengths between $p \times n_e$ and $p \times n_o$, where n_e and n_o are the extraordinary and the ordinary refractive indices of a uniaxially oriented phase, respectively. In practice, this means that the width of the reflection band is restricted to values smaller than 100 nm. It was recently demonstrated by Broer *et al.* that the reflection band can be broadened by creating a pitch gradient in the thickness direction of the cholesteric layer.[3] A gradient in UV intensity in the thickness direction of the film was used to provide a gradient in the rate of polymerization. Due to differences in reactivity between the cholesteric and the nematic monomers, an asymmetric distribution of the monomers was created over the thickness of the film. This resulted in a pitch gradient. Here we will demonstrate that photoisomerization of chiral copolymers can also be used to create gradients in the pitch. Two copolymers with different contents of chiral groups were used in this study: **B** (15 mol% menthone units) and **C** (30 mol% menthone units).

A 50 : 50%w/w mixture of **C** and the commercial nematic liquid crystal mixture E7 (Merck, Poole, UK) was introduced between two glass plates provided with rubbed orientation layers. A well-aligned cholesteric layer was obtained with a pitch reflecting blue light. In Fig. 12 (curve A) the wavelengths at half maximum of the reflection bands are shown as a function of irradiation time. From the figure it is clear that the reflection wavelength gradually shifts to longer wavelengths. The broadness of the reflection band is about 60–70 nm; it did not change dramatically during exposure.

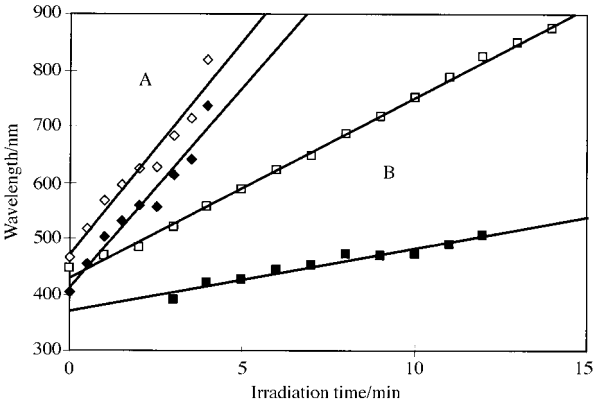

Fig. 12 Boundaries of the reflection band as a function of irradiation time. A: mixture of 50%w/w **C** and 50%w/w E7. Sample thickness 10 μm. Intensity: 5.6 mW cm^{-2}. B: mixture of 49%w/w **C**, 49%w/w E7 and 2% Tinuvin. Sample thickness 10 μm. Intensity: 2.8 mW cm^{-2}. The open symbols indicate the upper boundary of the reflection band and the filled symbols indicate the lower boundary of the reflection band. The boundaries were defined as the wavelengths at 50% of the maximum reflection.

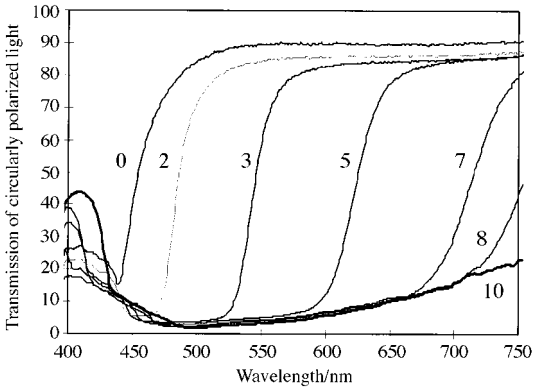

Fig. 13 Transmission spectra as a function of irradiation time. Sample: mixture of 49%w/w **C**, 49%w/w E7 and 2%w/w Tinuvin. Sample thickness 19 μm. Intensity: 2.8 mW cm^{-2}.

Curve B in Fig. 12 shows the results of the isomerization of a mixture containing 2%w/w UV absorber (Tinuvin 1130, Ciba Specialty Chemicals, Switzerland). Immediately after exposure the width of the reflection band starts to increase. The upper boundary of the reflection shifts faster than the lower boundary. Fig. 13 shows the reflection spectra of a thicker sample subjected to UV irradiation.

The low wavelength end remains at approximately the same position. The upper boundary of the reflection band gradually shifts through the spectrum. After 10 minutes exposure the reflection band spans the entire visible spectrum. When the irradiation time was continued for periods longer than 10 minutes the lower boundary also started to shift through the spectrum.

Apparently, the UV absorber creates a gradient in UV intensity throughout the layer. Due to the higher UV dose the isomerization is faster at the top of the layer than at the bottom and a gradient in the pitch is created.

These experiments show that the desired band broadening can be achieved. The mixture of **C** and E7 had a low viscosity. Due to diffusion of the compounds the pitch gradient gradually disappeared in time during storage. Polymer **B** reflected UV light without the introduction of E7. In this case, too, the UV absorber could be used to broaden the polymer's reflection band. Fig. 14 shows the transmission spectra of both left-handed and right-handed circularly polarized light for a broad band sample of **B**.

The cholesteric film transmits most of the right-handed circularly polarized light for the visible part of the spectrum. The left-handed circularly polarized light is largely reflected. The 1/4λ plate used for the measurements is optimized for light with a wavelength of 550 nm. By introducing achromatic 1/4λ plates the performance of the wide-band reflector will improve. In addition, it is expected that through careful

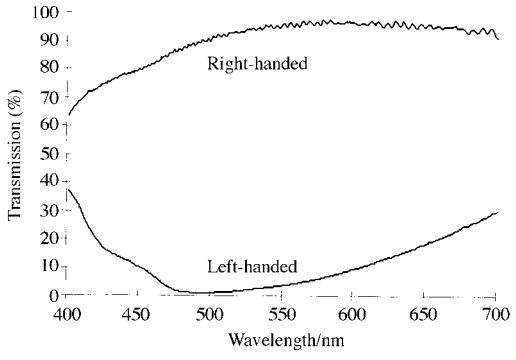

Fig. 14 Transmission spectra of left-handed and right-handed circularly polarized light. Sample: 98%w/w **B**, 2%w/w Tinuvin. Sample thickness: 10 μm. Intensity: 2.8 mW cm^{-2}.

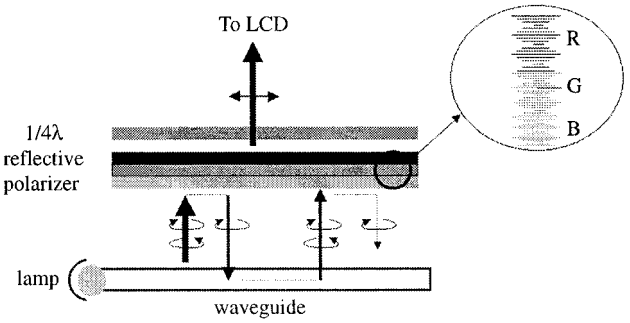

Fig. 15 Operating principle of a reflective polarizer. For explanation see text.

optimization of the experimental conditions the reflection and transmission characteristics can be further improved. Due to the vicinity of the glass transition temperature the wide band reflector prepared from **B** remains stable for several months at room temperature. Because the reflection is polarization selective for all wavelengths these layers can be used for application as a reflective polarizer.[52,4] In Fig. 15 the working principle of a reflective polarizer in an LCD is demonstrated.

The backlight emits non-polarized light. The reflective polarizer transmits one of the circular polarization directions. The 1/4λ plate converts the circularly polarized to the linearly polarized light required for the LCD. The other circular polarization direction is reflected into the backlight. In the backlight the light is partially depolarized and reflected to the reflective polarizer. In principle, the combination of reflection and depolarization can give rise to complete conversion of unpolarized light to polarized light. Compared with a classical polarizer, which is based on selective absorption of one polarization direction, a factor of two gain of light can be obtained.

4.3. Pitch reversal

In some cases the pitch of the helix can be reversed during irradiation. In high pitch regimes this has already been achieved in a single compound by Feringa *et al.*[36] We used a mixture of **1** and a non-photoreactive chiral compound with opposite twisting sense (R811) to achieve a reversal. This effect was shown to be useful to prepare a dual domain TN LCD with a reduced viewing angle dependence.[31]

It is interesting to study whether similar effects can be achieved in the range of visible light reflection with polymers. For that purpose monomer **2** was copolymerized with compound **5** in different ratios (Table 2). Due to the small temperature range of the cholesteric mesophase and the vicinity of the glass transition orientation of the polymers **F**–**I** was much more difficult than in the case of polymers **A**–**E**. Due to destabilization of the mesophase during irradiation, the temperature had to be well-chosen. The homopolymer **F** shows a 3 times smaller *HTP* than homopolymer **E**. In copolymer **G** the *HTP* of **2** is partly compensated by comonomer **5**. It reflects blue light. The reflection is shifted to the UV region during irradiation. Polymer **H** has a larger pitch. The reflection colors can now be shifted in the opposite direction (from long wavelengths to short wavelengths). Polymer **I** with the highest content of menthone derivative **2** showed a red reflecting cholesteric phase (at elevated temperatures). Using a 1/4λ plate and a polarizer it was checked that the twisting sense was opposite to that of polymers **F**–**H**. After irradiation with UV light the color vanished. Microscopic observation showed that the material had a nematic texture. Further irradiation led to the appearance of a red reflection with opposite twisting sense. Before irradiation compound **2** determined the pitch, and after irradiation compound **5**. Thus we developed a process in which

layers can be patterned with different colors and different twisting senses.

Using monomers with a higher helical twisting power the temperature range of the mesophase can be controlled more easily and a much larger pitch range will become accessible. Using the broad band technology it might even be possible to make a full mirror.

5. Conclusions

The potential of influencing the *HTP* by photoisomerization of the chiral dopant in liquid crystalline hosts appears to be large. The effects can be achieved in a wide pitch range. A number of potential applications are described. In particular menthone derivatives appear to be very suitable as chiral dopants. However, much research is still needed to increase the number of useful chiral compounds, to build a better understanding of the photochemistry and explore the possibilities offered by the materials.

Acknowledgements

The authors would like to acknowledge the contributions of J.-C. Galan, W. Nijssen, J. Steenbakkers and E. Neuteboom to this work.

References

1 N. Kurata, *1998 SID Int. Symp. Dig. Tech. Papers*, 43.
2 Brightness Enhancement Film, 3M product information.
3 D. J. Broer, J. Lub and G. N. Mol, *Nature*, 1995, **378**, 467.
4 D. J. Broer, J. A. M. M. van Haaren, G. N. Mol and F. Leenhouts, *Proc. 15th Int. Display Res. Conf. 1995*, *Hamamatsu* (*Japan*), 735.
5 D. L. Wortman, *1997 SID Int. Symp. Dig. Tech. Papers*, M-98.
6 Y. Dirix, H. Jagt, R. Hikmet and C. Bastiaansen, *J. Appl. Phys*., 1998, **83**, 2927.
7 M. Wenyon, W. Moleteni and P. Ralli, *1997 SID Int. Symp. Dig. Tech. Papers*, 691.
8 M. Honda, S. Hozumi and S. Kitayama, *Prog. Pac. Polym. Sci. 3*, *Proc. Pac. Polym. Conf. 3rd*, Springer-Verlag, Berlin, Heidelberg, 1995, p. 159.
9 T. J. Trout, J. J. Schmieg, W. J. Gambogi and A. M. Weber, *Adv. Mater*., 1998, **10**, 1219.
10 S. T. Wu, *Mater. Chem. Phys.*, 1995, **42**, 163.
11 M. Bosma, P. P. de Wit, A. Steenbergen and S. J. Picken, *1997 SID Int. Symp. Dig. Tech. Papers*, 679.
12 I. Heynderickx and D. J. Broer, *Mol. Cryst. Liq. Cryst*., 1991, **203**, 113.
13 S. Z. D. Cheng, F. Li, E. P. Savitski and F. W. Harris, *Trends Polym. Sci.*, 1997, **5**, 51.
14 C. D. Favre-Nicolin and J. Lub, *Adv. Mater.*, 1996, **8**, 1005.
15 K. Kawata, *IDW 1998*, *Proc. Fifth Int. Displ. Workshops* (*Kobe, Japan*), 109.
16 P. van de Witte, J. van Haaren, J. Tuijtelaars, S. Stallinga and J. Lub, *Jpn. J. Appl. Phys.*, 1999, **38**, 748.
17 H. Mori, Y. Itho, T. Nishiura, T. Nakamura and Y. Shinagara, *Jpn. J. Appl. Phys.*, 1997, **36**, 143.
18 P. van de Witte and J. Lub, *Liq. Cryst.*, 1999, **26**, 1039.
19 P. van de Witte, S. Stallinga and J. van Haaren, *Jpn. J. Appl. Phys*., in the press.
20 P. J. Collins and M. Hird, *Introduction to Liquid Crystals*, Taylor and Francis, London, 1997.
21 M. Schadt, H. Seiberle and A. Schuster, *Nature*, 1996, **381**, 212.
22 M. Schadt, K. Schmitt, V. Kozinkov and V. Chigrinov, *Jpn. J. Appl. Phys*., 1992, **31**, 2155.
23 K.-W. Lee, A. Lien, J. H. Stathis and S.-H. Paek, *Jpn. J. Appl. Phys.*, 1997, **36**, 3591.
24 M. Eich, J. H. Wendorff, B. Reck and H. Ringsdorf, *Makromol. Chem.*, *Rapid. Commun.*, 1987, **8**, 59.
25 T. Fuhrmann, M. Kunze, I. Lieker, A. Stracke and J. H. Wendorff, *Proc. SPIE*, 1996, **2852**, 42.
26 W. M. Gibbons, P. J. Shannon, S.-T. Sun and B. J. Swetlin, *Nature*, 1991, **351**, 49.
27 T. Ikeda and O. Tsutsumi, *Science*, 1995, **268**, 1873.
28 K. Ichimura, T. Seki, Y. Kawanishi, Y. Suzuki, M. Sakuragi and T. Tamaki, in *Photo-reactive Materials for Ultrahigh Density Optical Memory*, ed. M. Irie, Elsevier Science BV, Amsterdam, 1994, pp. 55–83.
29 M. Schadt, H. Seiberle, A. Schuster and S. M. Kelly, *Jpn. J. Appl. Phys*., 1995, **34**, L764.
30 W. M. Gibbons, T. Kosa, P. Palffy-Muhoray, P. J. Shannon and S. T. Sun, *Nature*, 1995, **377**, 43.
31 P. van de Witte, J. C. Galan and J. Lub, *Liq. Cryst*., 1998, **24**, 819.
32 M. Brehmer, J. Lub and P. van de Witte, *Adv. Mater.*, 1998, **10**, 1438.
33 P. van de Witte, M. Brehmer and J. Lub, *IDW 1998*, *Proc. Fifth Int. Displ. Workshops* (*Kobe*, *Japan*), 303.
34 F. Vicentini, J. Cho and L. C. Chien, *Liq. Cryst*., 1998, **24**, 483.
35 Y. Yokoyama, S. Uchida, Y. Yokoyama, T. Sagisaka, Y. Uchida and T. Inada, *Enantiomer*, 1998, **3**, 123.
36 B. N. Feringa, N. P. M. Huck and A. M. Schoevaars, *Adv. Mater.*, 1996, **8**, 68.
37 Y. Zhang and G. B. Schuster, *J. Org. Chem*., 1995, **60**, 7192.
38 C. Denekamp and B. L. Feringa, *Adv. Mater.*, 1998, **10**, 1080.
39 S. N. Yarmolenko, L. A. Kutulya, V. V. Vaschenko and L. V. Chepeleva, *Liq. Cryst.*, 1994, **16**, 877.
40 A. Yu. Bobrovski, N. I. Boiko and V. P. Shibaev, *Liq. Cryst.*, 1998, **25**, 393.
41 P. van de Witte, E. E. Neuteboom, M. Brehmer and J. Lub, *J. Appl. Phys.*, 1999, **85**, 7517.
42 M. Portugall, H. Ringsdorf and R. Zentel, *Makromol. Chem.*, 1982, **183**, 2311.
43 J. Lub, D. J. Broer, R. A. M. Hikmet and K. G. J. Nierop, *Liq. Cryst.*, 1995, **18**, 319.
44 J. Lub, J. H. van der Veen and E. van Echten, *Mol. Cryst. Liq. Cryst*., 1996, **287**, 205.
45 M. Portugall, H. Ringsdorf and R. Zentel, *Makromol. Chem.*, 1982, **183**, 2311.
46 R. Zentel, G. R. Strobl and H. Ringsdorf, *Macromolecules*, 1985, **18**, 960.
47 L. Cardillo, D. Swift and J. Merritt, *J. Imaging Sci. Technol*., 1998, **42**, 300.
48 J. Fergason, *Mol. Cryst.*, 1966, **1**, 293.
49 H. J. Eberle, A. Miller and F.-H. Kreuzer, *Liq. Cryst.*, 1989, **5**, 907.
50 E. M. Korenic, S. D. Jacobs, S. H. Faris and L. Li, *Color Res. Appl*., 1998, **23**, 210.
51 R. A. M. Hikmet and J. Lub, *Prog. Polym. Sci.*, 1996, **21**, 1165.

Paper 9/02593F